

Gear fault diagnosis using Autogram analysis

Advances in Mechanical Engineering
2018, Vol. 10(12) 1–11
© The Author(s) 2018
DOI: 10.1177/1687814018812534
journals.sagepub.com/home/ade



Adel Afia , Chemseddine Rahmoune and Djamel Benazzouz

Abstract

Rotary machines consist of various devices such as gears, bearings, and shafts that operate simultaneously. As a result, vibration signals have nonlinear and non-stationary behavior, and the fault signature is always buried in overwhelming and interfering contents, especially in the early stages. As one of the most powerful non-stationary signal processing techniques, Kurtogram has been widely used to detect gear failure. Usually, vibration signals contain a relatively strong non-Gaussian noise which makes the defective frequencies non-dominant in the spectrum compared to the discrete components, which reduce the performance of the above method. Autogram is a new sophisticated enhancement of the conventional Kurtogram. The modern approach decomposes the data signal by Maximal Overlap Discrete Wavelet Packet Transform into frequency bands and central frequencies called nodes. Subsequently, the unbiased autocorrelation of the squared envelope for each node is computed to select the node with the highest kurtosis value. Finally, Fourier transform is applied to that squared envelope to extract the fault signature. In this article, the proposed method is tested and compared to Fast Kurtogram for gearbox fault diagnosis using experimental vibration signals. The experimental results improve the detectability of the proposed method and affirm its effectiveness.

Keywords

Gear fault, Autogram, Kurtogram, diagnosis, autocorrelation, spectral kurtosis, defect

Date received: 11 July 2018; accepted: 15 October 2018

Handling Editor: Hui Ma

Introduction

Gears are often the most important part of rotating machines. They play a fundamental role in transmitting the power and the motion from one shaft to another. Therefore, any unexpected gear failure can reduce the performance of the industrial mechanism. Thence, it is necessary to detect the gear defect to avoid any serious failures. Several methods were used for the condition monitoring of rotating machinery such as temperature, vibration, and acoustic emission (AE).¹ Lately, gear fault diagnosis using vibration signals has been the subject of intensive studies in this field. Vibration signals carry many information about the state of the gearbox. Thus, a multitude of methods using those signals have been developed to extract the fault signature such as Fast Fourier Transform (FFT),² Cyclostationary Analysis,^{3,4} Cepstrum Analysis,⁵ Short-Time Fourier

Transform (STFT),⁶ Wigner–Ville Distribution,^{7–9} Wavelet Transform (WT),^{10–12} Hilbert–Huang Transform (HHT),^{13–15} Local Mean Decomposition (LMD),^{16–20} Empirical Mode Decomposition (EMD),^{20,21} Bayesian algorithms,²² Hilbert Empirical Wavelet Transform (HEWT),^{23,24} and Envelope Analysis.^{25,26}

In recent years, Envelope Analysis has gained much attention in gear fault diagnosis field. This method

Solid Mechanics and Systems Laboratory (LMSS), M'Hamed Bouguerra University of Boumerdès, Boumerdès, Algeria

Corresponding author:

Adel Afia, Solid Mechanics and Systems Laboratory (LMSS), M'Hamed Bouguerra University of Boumerdès, 35000 Boumerdès, Algeria.
Email: afiaadel19922015@gmail.com



separates the low-frequency disturbances around the mechanical resonance of the gear system using a band-pass filter. This is done using an amplitude demodulation technique and Fourier transform.²⁶ Unfortunately, the main problem of this tool is to find the best filtering frequency band.^{27,28} Consequently, Spectral Kurtosis (SK) is an important step in solving this problem. SK is an extension of the kurtosis in the frequency domain, where a suitable demodulation frequency band is located to select the maximum impulsivity in the data signal.²⁹ The SK-based STFT determines the center frequency and the length of the window where the SK value is maximized.³⁰ These values are represented by a second dimension color map called Kurtogram.^{29,31} As an alternative method, Fast Kurtogram (FK) has been suggested, in which the bandwidths are divided into rational ratios to apply a fast multi-rate technique to calculate the kurtosis value of the complex filtered signal.³⁰ Then, the most impulsive frequency band is selected.^{28–31} However, industrial equipments are complex systems consisting of various devices such as gearboxes, bearings, and shafts that operate simultaneously.³⁰ As a result, gear fault signatures are often covered by the machine natural frequencies and submerged by high non-Gaussian noise, such as large random impulses or very low noise ratio, making the defective frequencies non-dominant in the spectrum compared to discrete components.³⁰ Thence, in the previous case, FK will have many difficulties because the kurtosis value decreases as the transient's repetition rate increases.³⁰ A modern application, called Autogram, can manage this state by developing the conventional Kurtogram. This method is an effective tool for detecting the gear failure without depth knowledge. Autogram is based on unbiased autocorrelation (AC) to eliminate unrelated signal components such as noise and random impulse contents, and then improves periodic parts that are related to the fault signature.³⁰ Initially, the data signal is filtered and divided by WT into a dyadic tree structure to obtain different frequency bands and center frequencies.³⁰ However, the down-sampling operation reduces the ability to investigate the WT coefficients when there is a change in the starting point of the data signal.³⁰ Maximal Overlap Discrete Wavelet Transform (MODWT) overcomes the dyadic step. MODWT is a new enhancement of Discrete Wavelet Transform (DWT) without the down-sampling process,^{32–35} although MODWT has the same inconvenience as DWT. The bandwidth frequency used to decompose the signal is non-uniform.³⁵ Therefore, a substitute method has been developed called Maximal Overlap Discrete Wavelet Packet Transform (MODWPT) to provide a uniform frequency bandwidths and overcome time-variant transformation.^{32,35} MODWPT decomposes the original signal into many unique components with

different levels of resolution. MODWPT also allows the reconstruction of the original signal without losing any information and facilitates the monitoring of the gear state.³⁵ So, the principle of Autogram is defined according to these steps. First, MODWPT is used to decompose the vibration signal into several frequency bands and center frequencies called nodes.³⁰ Thereafter, the unbiased AC is calculated for the squared envelope for each node.³⁰ Autogram then determines the most appropriate frequency band to compute the kurtosis of the squared envelopes.³⁰ The kurtosis values are displayed in a color map, where the color scale is proportional to the kurtosis value, while the decomposition level and MODWPT frequency are presented in the vertical and horizontal axes, respectively.³⁰ Finally, the squared envelope, where the kurtosis value is maximized, is selected to extract the characteristic fault frequency using Fourier transform.³⁰

The aim of this article is to propose Autogram as a new method to enhance the gearbox fault diagnosis ability. Compared to FK, Autogram is more robust signal processing technique which could extract the fault signature even in noisy environment. Experimental results demonstrate the reliability and accuracy of the proposed method for early detection of a chipping fault.

Mathematical background

Autocorrelation

AC is a mathematical tool which compares a signal with a delayed version of itself. AC also allows the detection of repeated patterns in a signal such as a periodic signal disturbed by a lot of noise and then improves the periodic parts that are significantly related to the gear fault. The AC of a signal is calculated as follows:³⁰

- Find the value of the signal at a time t .
- Find the signal value at a time $t + \tau$.
- Multiple the two values together.
- Repeat the process.
- Calculate the average of all those products.

Mathematically, for a signal x , the unbiased AC of the squared envelope is calculated with this expression³⁰

$$\hat{R}_{XX}(\tau) = \frac{1}{N-q} \sum_{i=1}^{N-q} x(t_i)x(t_i + \tau) \quad (1)$$

with the delay factor is equal to $\tau = q/f_s$ and $q = 0, \dots, N-1$, where N is the length of the signal while f_s is the sampling frequency.

Spectral kurtosis and Kurtogram

Kurtosis detects the impulsivity faults related to rotating machines by computing the peakedness of the data signal as follows³⁰

$$Kurtosis = \frac{\sum_{i=1}^N (x(t_i) - \mu_x)^4}{\left[\sum_{i=1}^N (x(t_i) - \mu_x)^2 \right]^2} \quad (2)$$

where $x(t_i)$ presents the sample at time with $t_i = 1/f_s$, and μ_x is the mean value of the data signal.

The SK value is obtained by calculating the kurtosis value for each frequency band to extract its impulsive and non-stationary components, then find their location in the frequency domain as is expressed in³⁰

$$K_x(f) = \frac{\langle |Y(t_i, f)|^4 \rangle}{\langle |Y(t_i, f)|^2 \rangle^2} \quad (3)$$

with $Y(t_i, f)$ represent the STFT of the data signal while $\langle \rangle$ is the mean operator in time.

Kurtogram is the implementation result of these calculations for all possible combinations between frequencies and the window of STFT.

Combined squared envelope spectrum

The squared envelope spectrum (SES) is calculated for the nodes (n_{level}) with highest kurtosis values at every decomposed level. Thereafter, the normalized spectrums within 0 and 1 are combined by³⁰

$$SES(level) = \sum_{i=1}^{n_{level}} SES(i, level) \quad (4)$$

Maximal Overlap Discrete Wavelet Packet Transform

Continuous Wavelet Transform (CWT) is one of the most used signal processing methods. It gives a multi-time scale resolution. Each scale is considered as a frequency band to analyze the signal under several scales, and the CWT can be defined by^{11,34,36}

$$CWT(a, \tau) = \frac{1}{\sqrt{|a|}} \int_{-\infty}^{\infty} x(t) \psi^* \left(\frac{t - \tau}{a} \right) dt \quad (5)$$

where τ represents the translation parameter, while a is the dilation factor and it is called scale.

The main limit of CWT is the wide quantity of computation wavelet coefficients. DWT overcomes this limit by using a dyadic scale and translation parameter as defined in³⁶

$$DWT(a, \tau) = \frac{1}{\sqrt{2^j}} \int_{-\infty}^{\infty} x(t) \psi^* \left(\frac{t - 2^j k}{2^j} \right) dt \quad (6)$$

where 2^j and $2^j k$ replace the dilation and translation parameters, respectively.

The DWT decomposes the signal using a high-pass and low-pass filters to analyze the high-frequency bands [*Details* D_j] and the low-frequency bands [*Approximations* A_j], respectively, at level j . The decomposition process is defined in³⁶

$$x(t) = A_J + \sum_{j \leq J} D_j \quad (7)$$

Figure 1 gives a better illustration of the decomposition process.

The motivation for formulating the Discrete Wavelet Packet Transform (DWPT) is essentially to overcome the main problem of DWT. Unless DWT, DWPT decomposes both the detail and approximation coefficients at each levels to obtain more information as follows³⁵

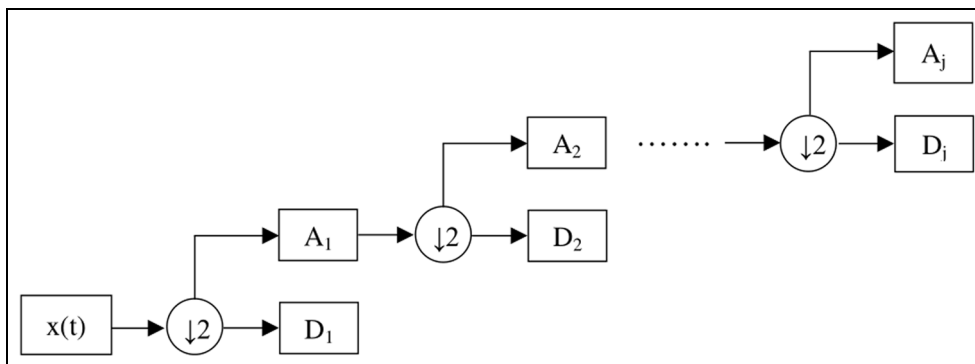


Figure 1. Decomposition process using DWT.

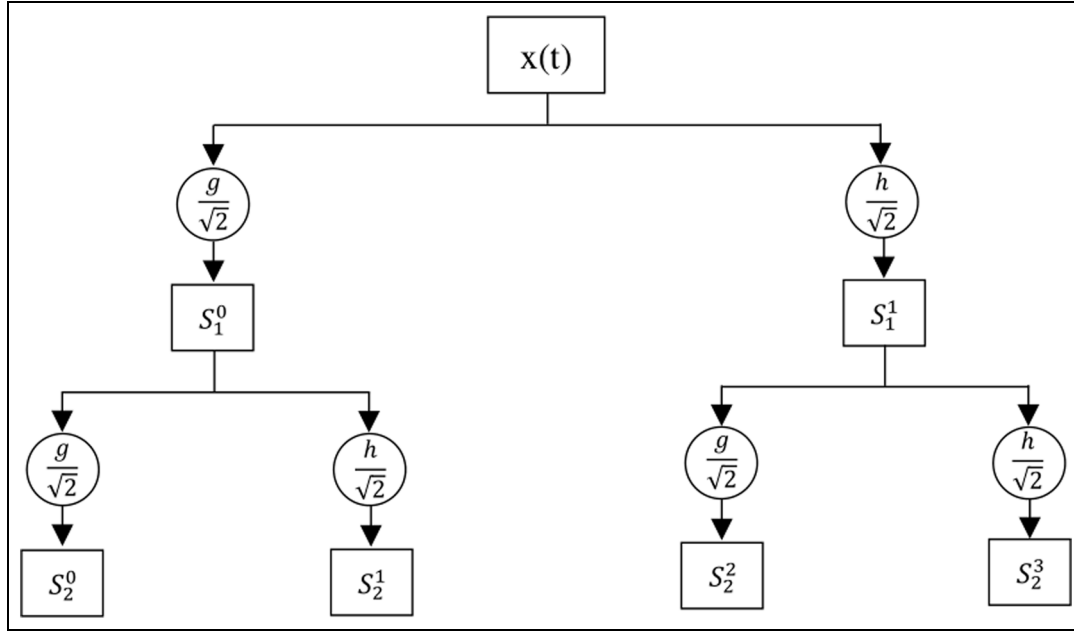


Figure 2. Two levels of the MODWPT decomposition.

$$s_j^{2z}(k) = \sum_{n=-\infty}^{+\infty} g(n)s_{j-1}^z(2k-n) \quad (8)$$

$$s_j^{2z+1}(k) = \sum_{n=-\infty}^{+\infty} h(n)s_{j-1}^z(2k-n) \quad (9)$$

with z is the node number and $z = 2m$, where $m \in \mathbb{N}$ and $m \leq 2^{j-1} - 1$ at level j . s_0^0 presents the original signal and $s_j^z(k)$ is the decomposition packet coefficients of the higher frequency bands, while h and g are the wavelet filters and their properties are given in³⁵

$$\sum_{n=-\infty}^{+\infty} g(n) = \sqrt{2}, \quad \sum_{n=-\infty}^{+\infty} g^2(n) = 1, \quad \sum_{n=-\infty}^{+\infty} g(n)h(n) = 0 \quad (10)$$

$$\sum_{n=-\infty}^{+\infty} h(n) = 0, \quad \sum_{n=-\infty}^{+\infty} h^2(n) = 1, \quad \sum_{n=-\infty}^{+\infty} h(n)g(n) = 0 \quad (11)$$

Although both DWT and DWPT have some disadvantages like time-variant property due to the down-sampling process, MODWPT overcomes those drawbacks by dispensing that dyadic step as shown in Figure 2. The MODWPT decomposition coefficients are expressed as follows³⁵

$$s_j^{2z}(k) = \frac{1}{\sqrt{2}} \sum_{n=-\infty}^{+\infty} g(n)s_{j-1}^z(k-n) \quad (12)$$

$$s_j^{2z+1}(k) = \frac{1}{\sqrt{2}} \sum_{n=-\infty}^{+\infty} h(n)s_{j-1}^z(k-n) \quad (13)$$

Autogram

As detailed in Moshrefzadeh and Fasana,³⁰ Autogram could be described in the following steps:

Step 1: The data signal is filtered and decomposed using MODWPT into frequency bands and center frequencies called nodes. MODWPT is a sophisticated version of the DWPT without the down-sampling process.^{32,35} The down-sampling step is the main limit of DWPT because of the sensitivity of the starting point selection in a time data, for instance, a change in the starting point can give quite different results.³⁰ MODWPT is also used as a filter to analyze the data signal at all decomposition levels. Each filtered data correspond to a frequency band and a center frequency (node).

Step 2: Autogram uses the periodicity of the autocovariance function. In this step, the unbiased AC is calculated on the squared envelope of the filtered signal using equation (1). AC eliminates all uncorrelated parts of the signal such as noise and random impulsive components and improves all periodic components that are related to gear failure.³⁰ Also, AC offers more advantages since it is done on each node separately to remove any random impulsive part that defines a very high kurtosis.³⁰

Step 3: The aim in this step is to select an appropriate frequency band for the demodulation signal for an effective gear fault diagnosis. In this step, the kurtosis is evaluated on the unbiased AC of the squared envelope for each level and frequency band (nodes). Kurtosis values for all nodes are displayed

in a color map, where the color scale is proportional to the kurtosis value, while the decomposition level and MODWPT frequency are presented in the vertical and horizontal axes, respectively.

Equations (14) to (16) give a three modified equations of the conventional kurtosis in order to measure the impulsivity of AC for each node obtained above³⁰

$$Kurtosis(X) = \frac{\sum_{i=1}^{\frac{N}{2}} [\hat{R}_{XX}(i) - \min(\hat{R}_{XX}(\tau))]^4}{\left[\sum_{i=1}^{\frac{N}{2}} [\hat{R}_{XX}(i) - \min(\hat{R}_{XX}(\tau))]^2 \right]^2} \quad (14)$$

$$Kurtosis_u(X) = \frac{\sum_{i=1}^{\frac{N}{2}} |\hat{R}_{XX}(i) - \bar{X}_T(i)|_+^4}{\left[\sum_{i=1}^{\frac{N}{2}} |\hat{R}_{XX}(i) - \bar{X}_T(i)|_+^2 \right]^2} \quad (15)$$

$$Kurtosis_l(X) = \frac{\sum_{i=1}^{\frac{N}{2}} |\hat{R}_{XX}(i) - \bar{X}_T(i)|_-^4}{\left[\sum_{i=1}^{\frac{N}{2}} |\hat{R}_{XX}(i) - \bar{X}_T(i)|_-^2 \right]^2} \quad (16)$$

Only positive and negative values are accepted while the other are converted to zero, and \bar{X}_T is the threshold level and it is defined as follows³⁰

$$\bar{X}_T(i) = \frac{1}{k} \sum_{j=1}^{i+k-1} \hat{R}_{XX}(i) \quad (17)$$

where k is the length of the windowed signal.

As we mentioned in the previous step, AC eliminates all the uncorrelated parts in the signal such as noise and random impulsive which may ineffectively assigns very high kurtosis. Therefore, the node with the highest kurtosis value is selected as an optimal frequency band for the demodulation signal.

Step 4: Fourier transform is applied to the squared envelope with the highest kurtosis value to extract the feature frequency, which is associated to the gear fault.

Figure 3 summarizes the four previous steps.

Experimental description

The vibration signals have been provided from CETIM, France.³⁷ They were delivered from a single-stage speed reducer as shown in Figure 4. The gearbox is composed of a pinion and a gear with 20 and 21 teeth, respectively. The rotation frequency of the input

shaft is equal to $f_{r1} = 16.67$ Hz and $f_{r2} = 15.87$ Hz on the output shaft, while the meshing frequency is equal to $f_{mesh} = 333.33$ Hz with 20 kHz as a sampling frequency.

The gearbox system was operating for 24 h over 24 h, and experimental vibration signals were collected for 13 days, except the first day (no data acquisition), until we were close to the tooth break as illustrated in the expert report (Table 1). The dimensions of gears in addition to the operating conditions (speed, torque) have been adjusted to obtain chipping fault over the entire width of a tooth. During experience, the test bench has been stopped every day to appraise the gear state.

Figure 5 shows the faultless and the faulty tooth in the pinion, while Table 2 shows the different dynamic and geometrical parameters of the gear system.

Results and discussion

The data sets provided by CETIM, France,³⁷ will be used to evaluate the performance of the proposed method by comparing the results with another signal processing technique. The comparison was provided with FK to prove the effectiveness of the suggested approach.

Table 1 gives the expert report and there is no data acquisition for the first day. Our purpose is to recognize the defect from the vibration signals collected before the tooth is broken.

The experimental signals for 2nd, 7th, and 10th days are shown in Figure 6. It can be seen that it is not possible to detect the gear failure only by looking at the waveform, since the fault impulses are masked by the noise.

The signals generated by a defective gear have two important characteristics: a wide frequency and a very low energy compared to the total energy of the signal, so it is difficult to detect the chipping defect through a simple conventional signal processing technique.

To overcome this problem, we first applied FK on the vibration signals recorded with a sampling frequency of 20 kHz. Figures 7 and 8 show the FK and the corresponding envelope spectrum of the filtered signal for days 2, 7, and 10, respectively. Figure 7(b) displays the color map of FK for 7th day, the bandwidth and center frequency are equal to 2500 and 8750 Hz, respectively, while Figure 8(b) displays the spectrum of that band. From Figure 8(b), we notice that it is not possible to extract the defect signature using FK. This is due to the nature of the impulses that are converted by noise. Whereas from Figure 8(c), we could obviously view the appearance of a new frequency that effectively corresponds to the input shaft frequency $f_{r1} = 16.67$ Hz with $2f_{r1}$ is its harmonics.

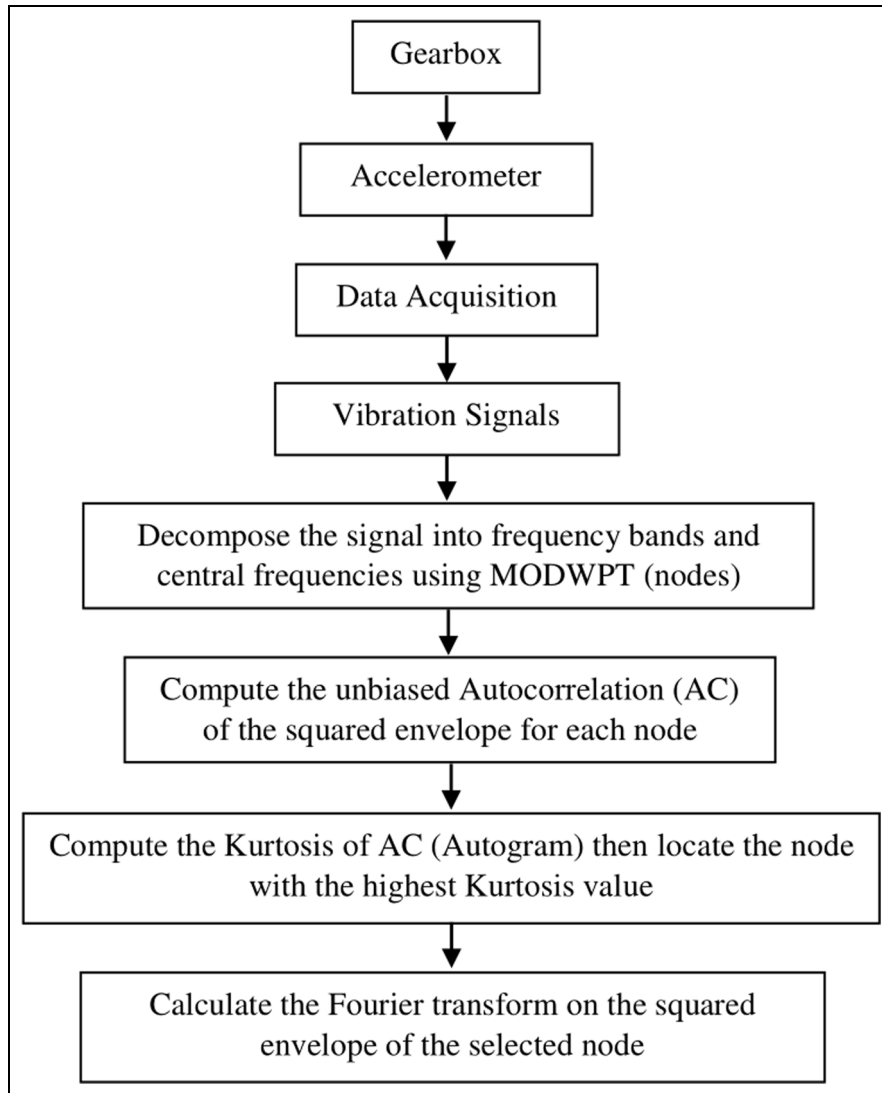


Figure 3. Flowchart for the new proposed method.

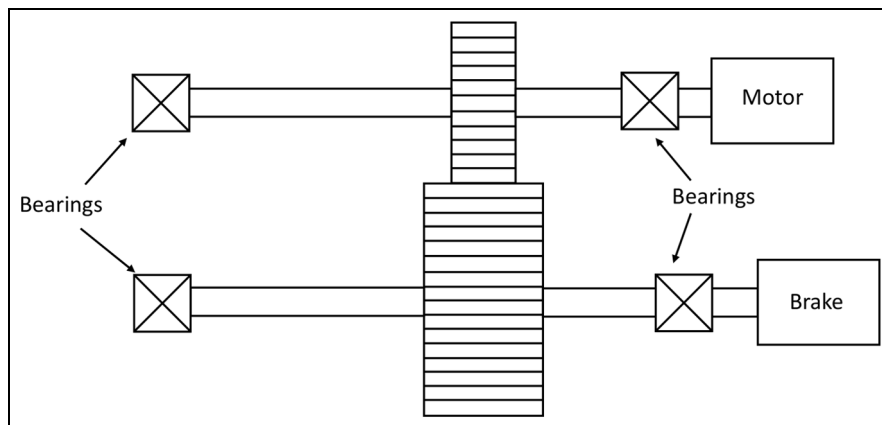


Figure 4. Schematic representation of the test rig CETIM.

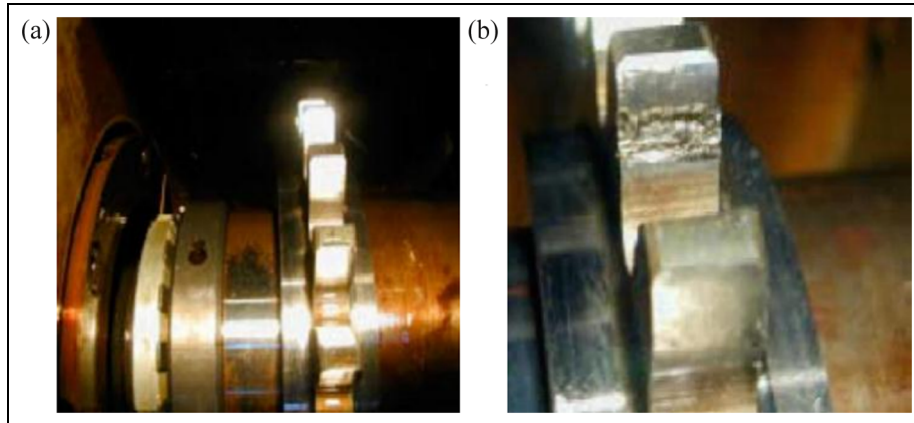


Figure 5. Pictures of the pinion from CETIM test rig: (a) without defect and (b) with defect.

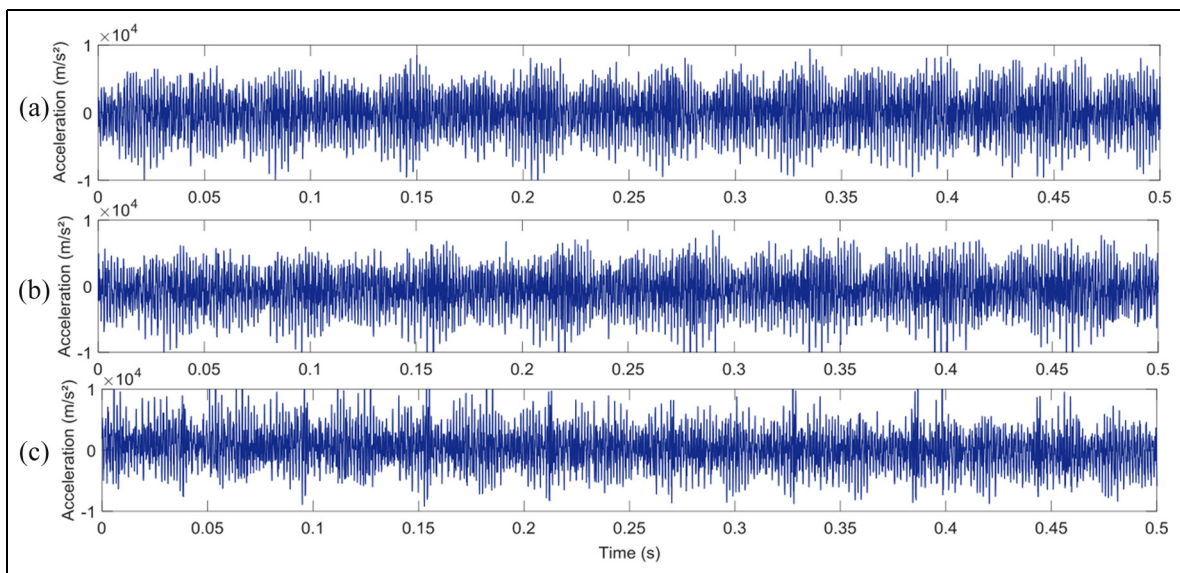


Figure 6. Analyzed vibration signals of (a) 2nd, (b) 7th, and (c) 10th days.

The results obtained indicate that we could only detect the gear defect using FK after the 10th day, while the expert report (Table 1) indicates that we could detect it before that.

Thereafter, the proposed “Autogram” method is applied to the same data signals. The results are shown in Figures 9 and 10. Unlike FK, a smaller frequency bandwidth is located (156.25 Hz) in the 7th day as shown in Figure 9(b). The corresponding squared envelope spectrum for the 7th day is shown in Figure 10(b). We can see that the squared envelope spectrum immediately indicates a typical modulation which actually corresponds to the input shaft rotation speed, $f_{r1} = 16.67$ Hz (Figure 10(b)). It is also possible to notice the presence of the same frequency at the 10th day, when the width of the chipping tooth has evolved

Table I. The expert report.

Days	Observations
1	No acquisition
2	First day of acquisition, no anomaly
3	No anomaly
4	////
5	////
6	////
7	Chipping tooth (1/2 width)
8	No evolution
9	Beginning of chipping with 15/16 width of the tooth
10	Evolution of chipping tooth (15/16 width)
11	////
12	////
13	Chipping over all the width of tooth

//// : same thing as the previous day

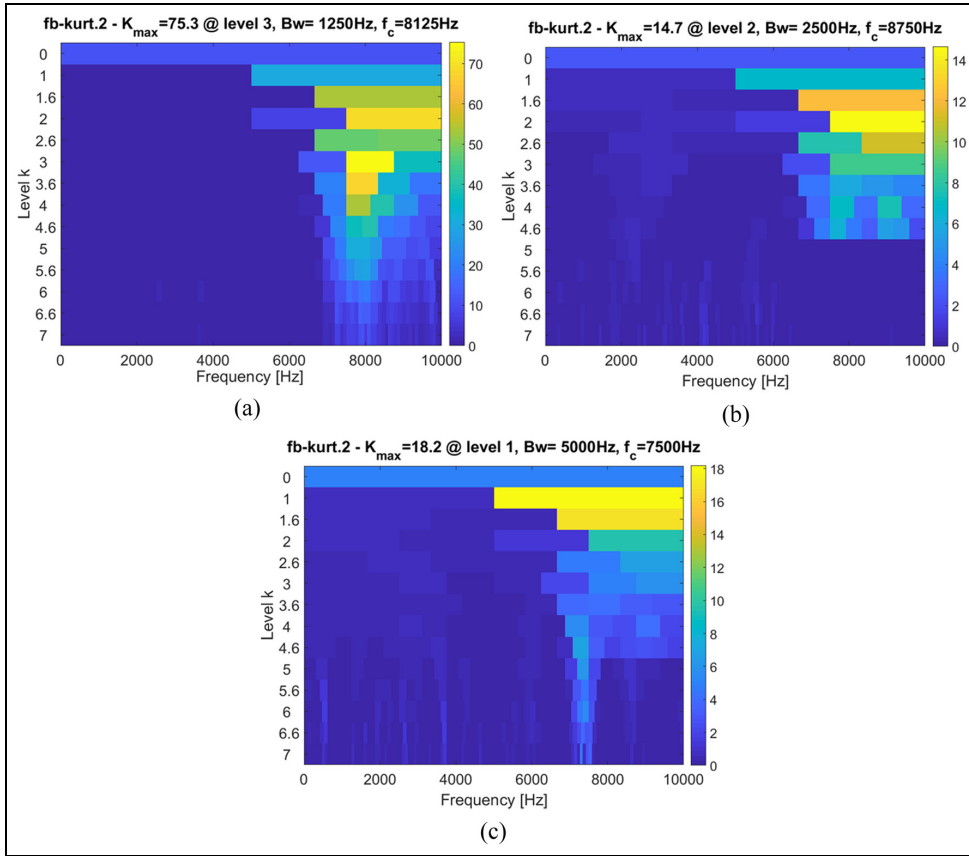


Figure 7. Fast Kurtogram of the vibration signals for (a) 2nd, (b) 7th, and (c) 10th days.

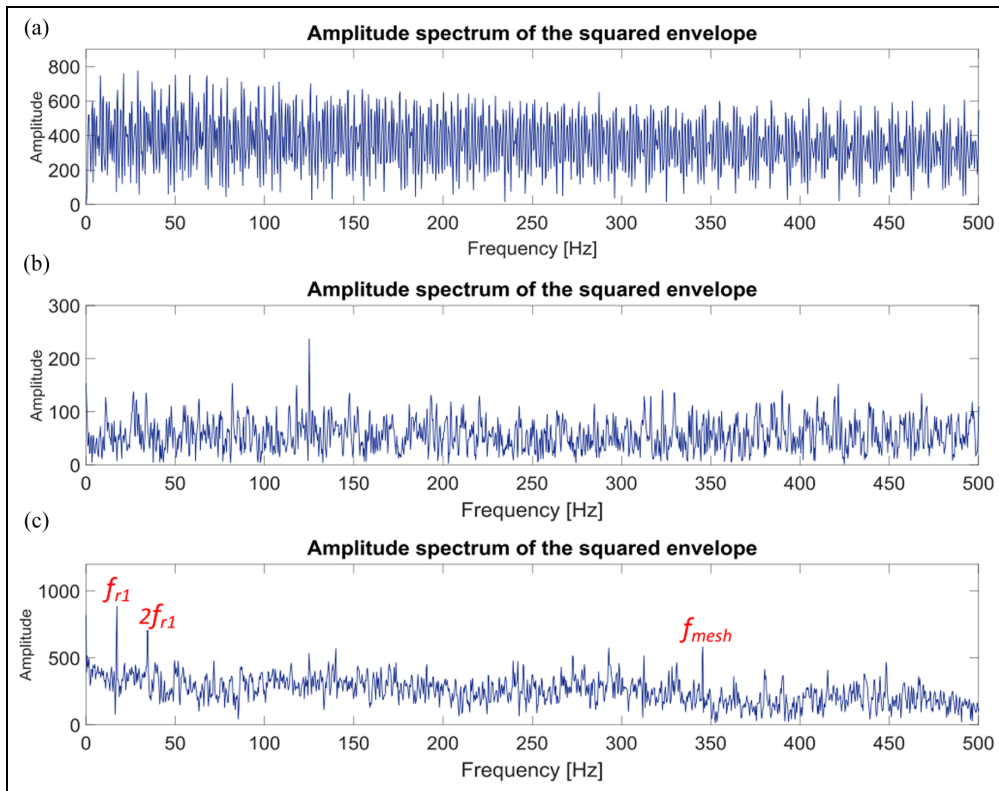


Figure 8. The envelope spectrum provided by the Fourier transform for (a) 2nd, (b) 7th, and (c) 10th days.

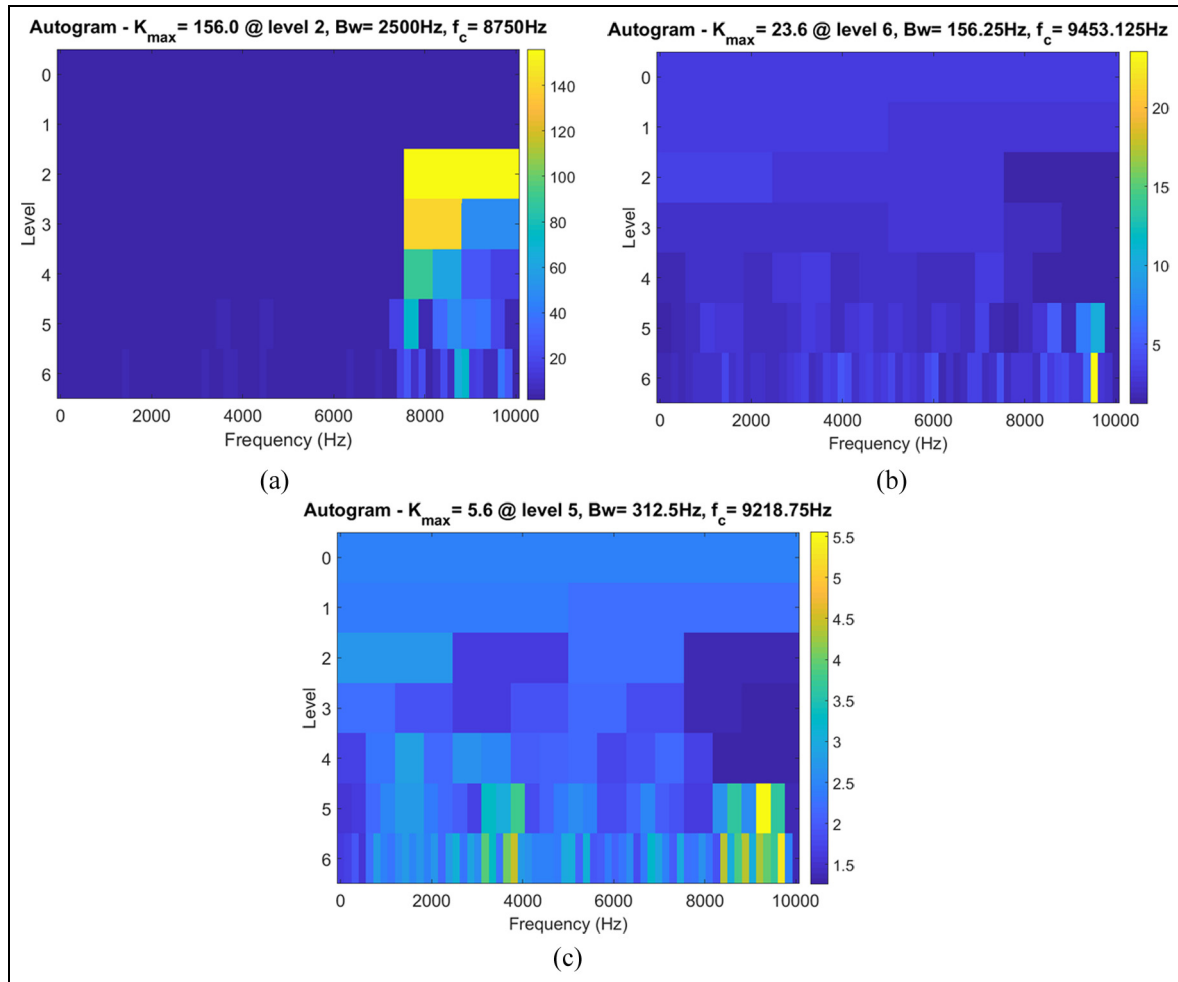


Figure 9. Autogram of the vibration signals for (a) 2nd, (b) 7th, and (c) 10th days.

Table 2. Dynamic and geometrical parameters of the gear system.

Parameter	Pinion	Gear
Speed, r/min	1000	952
Number of teeth	20	21
Face width, m	0.015	0.03
Shaft diameter, m	0.092	0.110
Module, m	0.01	0.01
Mass, N	36	80
Drive torque, N m	200	

up to 15/16 of the entire width (Figure 10(c)), which confirms the robustness and effectiveness of the proposed method compared to FK.

Conclusion

Gear fault diagnosis requires a powerful non-stationary vibration signal analysis tool to extract the fault signature buried in strong background noise. FK has a

strong ability to detect the gear failure even in noisy environment. However, a robust signal processing technique is still required when the vibration signals are covered by strong non-Gaussian noise. Therefore, a new method named Autogram is proposed to reduce the influence of noise, which covers the gear defect from a raw data. In contrast with Kurtogram, this new method finds the perfect frequency band for demodulation to allow a better feature extraction. First, the data signal is decomposed by MODWPT into different frequency bands and center frequencies (nodes). Subsequently, the unbiased AC of the squared envelope is computed for each node to decrease the uncorrelated random noise. Thereafter, Autogram selects the node with the highest kurtosis value. Finally, Fourier transform is applied on the optimal selected frequency band to extract the fault signature. Experimental data sets with faultless and a faulty gearbox were utilized and compared with FK to test the accuracy of the suggested approach. The experimental results confirm the

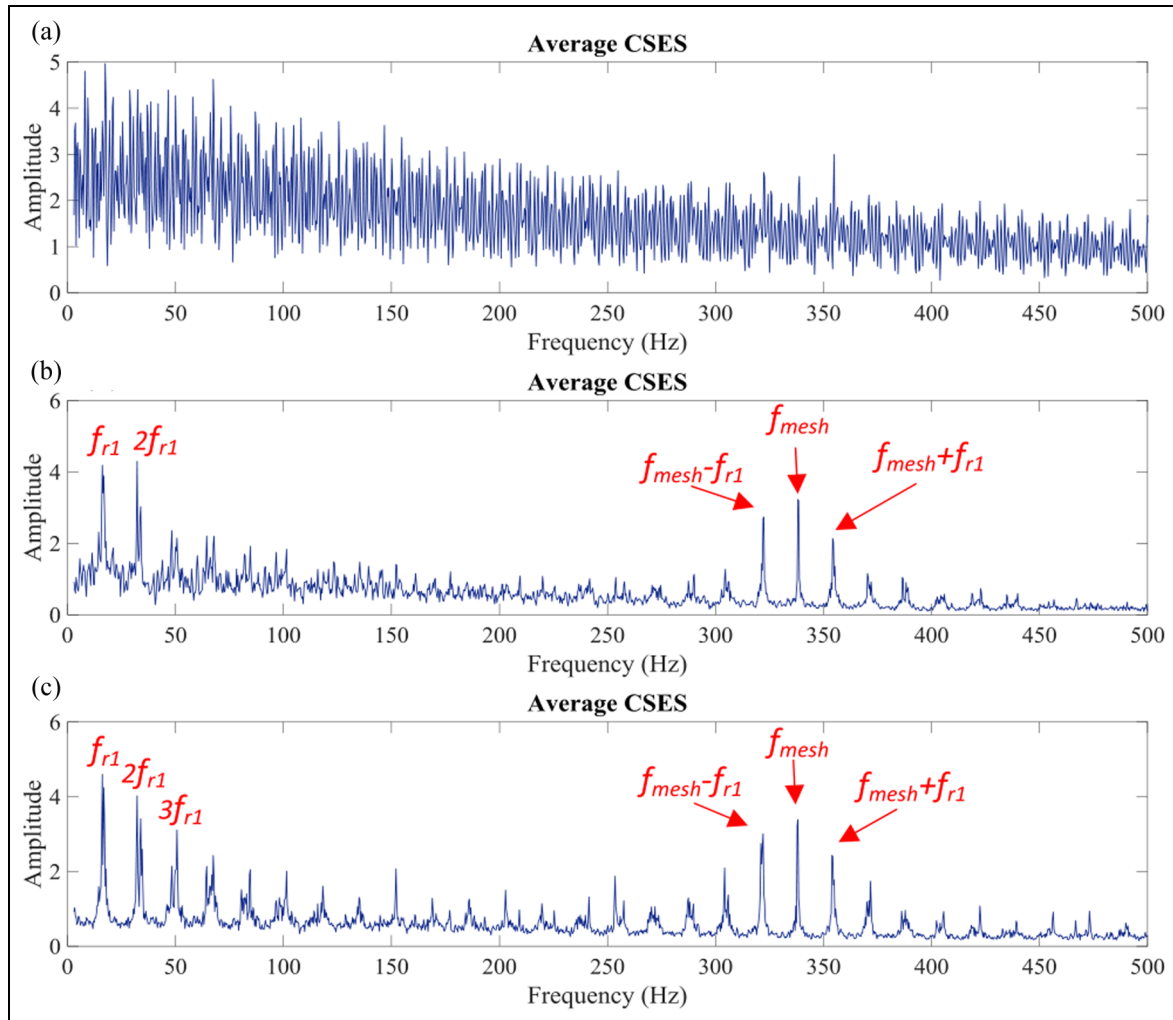


Figure 10. The squared envelope spectrum provided by the Fourier transform for (a) 2nd, (b) 7th, and (c) 10th days.

effectiveness of our method in the identification of gear failure even in the presence of non-Gaussian noise.


Declaration of conflicting interests

The author(s) declared no potential conflicts of interest with respect to the research, authorship, and/or publication of this article.

Funding

The author(s) received no financial support for the research, authorship, and/or publication of this article.

ORCID iD

Adel Afia  <https://orcid.org/0000-0002-7602-0951>

References

1. Wang T, Chu F, Han Q, et al. Compound faults detection in gearbox via meshing resonance and spectral kurtosis methods. *J Sound Vib* 2017; 392: 367–381.
2. Betta G, Liguori C, Paolillo A, et al. A DSP-based FFT-analyzer for the fault diagnosis of rotating machine based on vibration analysis. *IEEE T Instrum Meas* 2002; 51: 1316–1322.
3. Capdessus C, Sidahmed M and Lacoume L. Cyclostationary processes: application in gear faults early diagnosis. *Mech Syst Signal Pr* 2000; 14: 371–385.
4. Lin J and Zuo MJ. Extraction of periodic components for gearbox diagnosis combining wavelet filtering and cyclostationary analysis. *J Vib Acoust* 2004; 126: 449–451.
5. El Badaoui M, Guillet F and Daniere J. New applications of the real cepstrum to gear signals including definition of a robust fault indicator. *Mech Syst Signal Pr* 2004; 18: 1031–1046.
6. Huizhong G, Lin L, Xiaoguang C, et al. Feature extraction and recognition for rolling element bearing fault utilizing short-time Fourier transform and non-negative matrix factorization. *Chin J Mech Eng* 2015; 28: 96–105.
7. Staszewski WJ, Worden K and Tomlinson GR. Time-frequency analysis in gearbox fault detection using Wigner–Ville distribution and pattern recognition. *Mech Syst Signal Pr* 1997; 11: 673–692.

8. Baydar N and Ball A. A comparative study of acoustic and vibration signals in detection of gear failures using Wigner–Ville distribution. *Mech Syst Signal Pr* 2001; 15: 1091–1107.
9. Tang B, Liu W and Song T. Wind turbine fault diagnosis based on Morlet wavelet transformation and Wigner–Ville distribution. *Renew Energ* 2010; 35: 2862–2866.
10. Wang WJ and McFadden PD. Application of wavelets to gearbox vibration signals for fault detection. *J Sound Vib* 1996; 192: 927–939.
11. Zheng H, Li Z and Chen X. Gear fault diagnosis based on continuous wavelet transform. *Mech Syst Signal Pr* 2002; 16: 447–457.
12. Peng ZK and Chu FL. Application of the wavelet transform in machine condition monitoring and fault diagnostics: a review with bibliography. *Mech Syst Signal Pr* 2004; 18: 199–221.
13. Yu D, Yang Y and Cheng J. Application of time–frequency entropy method based on Hilbert–Huang transform to gear fault diagnosis. *Measurement* 2007; 40: 823–830.
14. Wu TY, Chen J and Wang C. Characterization of gear faults in variable rotating speed using Hilbert–Huang transform and instantaneous dimensionless frequency normalization. *Mech Syst Signal Pr* 2012; 30: 103–122.
15. Cheng G, Cheng Y, Shen L, et al. Gear fault identification based on Hilbert–Huang transform and SOM neural network. *Measurement* 2013; 46: 1137–1146.
16. Chen B, He Z, Chen X, et al. A demodulating approach based on local mean decomposition and its applications in mechanical fault diagnosis. *Meas Sci Technol* 2011; 22: 055704.
17. Cheng J, Zhang K and Yang Y. An order tracking technique for the gear fault diagnosis using local mean decomposition method. *Mech Mach Theory* 2012; 55: 67–76.
18. Cheng J, Yang Y and Yang Y. A rotating machinery fault diagnosis method based on local mean decomposition. *Digit Signal Process* 2012; 22: 356–366.
19. Liu WY, Zhang WH, Han JG, et al. A new wind turbine fault diagnosis method based on the local mean decomposition. *Renew Energ* 2012; 48: 411–415.
20. Thameur K, Marc T, Raynald G, et al. Comparison between the efficiency of L.M.D and E.M.D algorithms for early detection of gear defects. *J Mech Struct Mach* 2013; 14: 121–127.
21. Huang NE, Shen Z, Long SR, et al. The empirical mode decomposition and the Hilbert spectrum for nonlinear and non-stationary time series analysis. *P Roy Soc A: Math Phy* 1998; 454: 903–995.
22. Jiang R, Yu J and Makis V. Optimal Bayesian estimation and control scheme for gear shaft fault detection. *Comput Ind Eng* 1998; 454: 903–995.
23. Merainani B, Benazzouz D and Rahmoune C. Early detection of tooth crack damage in gearbox using empirical wavelet transform combined by Hilbert transform. *J Vib Control* 2015; 23: 1623–1634.
24. Merainani B, Benazzouz D and Rahmoune C. A novel gearbox fault feature extraction and classification using Hilbert empirical wavelet transform, singular value decomposition, and SOM neural network. *J Vib Control* 2017; 24: 2512–2531.
25. Kang M, Kim J, Wills L, et al. Time-varying and multi-resolution envelope analysis and discriminative feature analysis for bearing fault diagnosis. *IEEE T Ind Electron* 2015; 62: 1.
26. Abboud D, Antoni J, Sieg-Zieba S, et al. Envelope analysis of rotating machine vibrations in variable speed conditions: a comprehensive treatment. *Mech Syst Signal Pr* 2017; 84: 200–226.
27. Guo Y, Wu X, Na J, et al. Incipient faults identification in gearbox by combining Kurtogram and independent component analysis. *Mech Mater* 2015; 764–765: 309–313.
28. Moshrefzadeh A, Fasana A and Garibaldi L. Using unbiased autocorrelation to enhance Kurtogram and envelope analysis results for rolling element bearing diagnostics. In: *Proceedings of the international conference on surveillance*, Fes, Morocco, 22–24 May 2017, pp. 1–8.
29. Rahmoune C and Benazzouz D. Early detection of pitting failure in gears using a spectral kurtosis analysis. *Mech Ind* 2012; 13: 245–254.
30. Moshrefzadeh A and Fasana A. The Autogram: an effective approach for selecting the optimal demodulation band in rolling element bearings diagnosis. *Mech Syst Signal Pr* 2018; 105: 294–318.
31. Barszcz T and Jaboski A. A novel method for the optimal band selection for vibration signal demodulation and comparison with the Kurtogram. *Mech Syst Signal Pr* 2011; 25: 431–451.
32. Yang Y, He Y, Cheng J, et al. A gear fault diagnosis using Hilbert spectrum based on MODWPT and a comparison with EMD approach. *Measurement* 2009; 42: 542–551.
33. Khalighi S, Sousa T, Oliveira D, et al. Efficient feature selection for sleep staging based on maximal overlap discrete wavelet transform and SVM. In: *Proceedings of the annual international conference of the IEEE engineering in medicine and biology society*, Boston, MA, 30 August–3 September 2011, pp.2225–5046. New York: IEEE.
34. Alarcon-Aquino V and Barria JA. Change detection in time series using the maximal overlap discrete wavelet transform. *Lat Am Appl Res* 2009; 39: 145–152.
35. Alves DK, Costa FB, Araujo Ribeir RL, et al. Real-time power measurement using the maximal overlap discrete wavelet-packet transform. *IEEE T Ind Electron* 2017; 64: 3177–3187.
36. Wu JD and Hsu CC. Fault gear identification using vibration signal with discrete wavelet transform technique and fuzzy-logic inference. *Expert Syst Appl* 2009; 36: 3785–3794.
37. Mahgoun H, Bekka RE and Felkaoui A. Gearbox fault diagnosis using ensemble empirical mode decomposition (EEMD) and residual signal. *Mech Ind* 2012; 13: 33–44.